Poswillo D. 1975. Hemorrhage in development of the face. Birth Defects Orig Artic Ser 11:61–81.

Rollnick BR, Kaye CI. 1983. Hemifacial microsomia and variants: Pedigree data. Am J Med Genet 15:233–253.

Schinzel AA, Smith DW, Miller JR. 1979. Monozygotic twinning and structural defects. J Pediatr 95:921–930.

Stoll C, Viville B, Treisser A, Gasser B. 1998. A family with dominant oculoauriculovertebral spectrum. Am J Med Genet 78:345–349.

Townes PL, Brocks ER. 1972. Hereditary syndrome of imperforate anus with hand, foot, and ear anomalies. J Pediatr 81:321–326.

ELSEVIER

Partial Deletion of *LIS1*: A Pitfall in Molecular Diagnosis of Miller-Dieker Syndrome

Kosuke Izumi, MD, Gen Kuratsuji, MD, Kazushige Ikeda, MD, Takao Takahashi, MD, and Kenjiro Kosaki, MD

Miller-Dieker syndrome represents a microdeletion syndrome spanning the *LIS1* locus at 17p13.3, the deletion of which leads to lissencephaly. A fluorescence in situ hybridization study using an *LIS1* probe is considered the standard laboratory diagnostic method for Miller-Dieker syndrome. This report documents a Miller-Dieker syndrome patient who tested normal when a commercially available *LIS1* fluorescence in situ hybridization study probe was used but was later demonstrated to have a partial deletion of the *LIS1* locus. The present case exemplifies a major shortcoming of commercially available fluorescence in situ hybridization studies for the diagnosis of microdeletion syndromes such as Miller-Dieker syndrome: that is, relatively small deletion can potentially remain undetected.

Izumi K, Kuratsuji G, Ikeda K, Takahashi T, Kosaki K. Partial deletion of *LIS1*: A pitfall in molecular diagnosis of Miller-Dieker syndrome. Pediatr Neurol 2007;36: 258-260.

Introduction

Miller-Dieker syndrome is characterized by dysmorphic features including a prominent forehead and vertical furrowing of the forehead upon crying and lissencephaly accompanied by severe developmental delays and seizures [1-3]. Miller-Dieker syndrome represents a microdeletion syndrome spanning the *LIS1* locus at 17p13.3, the deletion of which leads to lissencephaly [4,5]. Confirmation of a clinical diagnosis using either cytogenetic or molecular techniques allows clinicians to provide the family with prognostic information and anticipatory medical care.

A recently published standard textbook of pediatric neurology states that "chromosome analysis identifies visible deletions of 17p13.3 in approximately 60% to 70% of patients, and fluorescence in situ hybridization detects deletions in the remaining patients" [6]. Thus, a fluorescence in situ hybridization study using an *LIS1* probe is considered the standard laboratory diagnostic method for Miller-Dieker syndrome [7]. The present report documents a Miller-Dieker syndrome patient who tested normal when a commercially available *LIS1* fluorescence in situ hybridization study probe was used but was later demonstrated to have a partial deletion of the *LIS1* locus.

Case Report

The proband was a product of a healthy nonconsanguineous Japanese couple. The familial history was unremarkable. Intrauterine growth retardation was observed at 23 weeks of gestation. When polyhydramnios became evident at 30 weeks of gestation, an amniocentesis was performed. A G-band analysis of an amniotic fluid culture revealed a structural abnormality in chromosome 17 (46,XX,?17p), but further details were not available. The female patient was delivered at 36 weeks of gestation; her Apgar scores were 7 and 9 at 1 and 5 minutes, respectively. She presented with several dysmorphic features including micrognathia, midface hypoplasia, a thin vermilion border, retrognathia, an aberrant palmar crease pattern, and hypoplasia of the labia minor. Upon crying, she exhibited vertical furrows on her forehead. A magnetic resonance imaging study of her brain revealed global agyria with an hourglass configuration (Grade 1 [8] lissencephaly), a septum pellucidum cyst, and an abnormal distribution of gray and white matter in the cerebral hemispheres (Fig 1). Based on these characteristic facial features, including the vertical forehead furrows upon crying, and the magnetic resonance imaging findings, including severe lissencephaly, she was clinically diagnosed as having Miller-Dieker syndrome.

From Department of Pediatrics, Keio University School of Medicine, Tokyo, Japan.

Communications should be addressed to:
Dr. Kosaki; Department of Pediatrics; Keio University School of Medicine; 35 Shinanomachi, Shinjuku-ku; Tokyo. 160-8582. Japan.
E-mail: kkosaki@sc.itc.keio.ac.jp
Received August 7, 2006; accepted November 27, 2006.

doi:10.1016/j.pediatrneurol.2006.11.015 • 0887-8994/07/$—see front matter

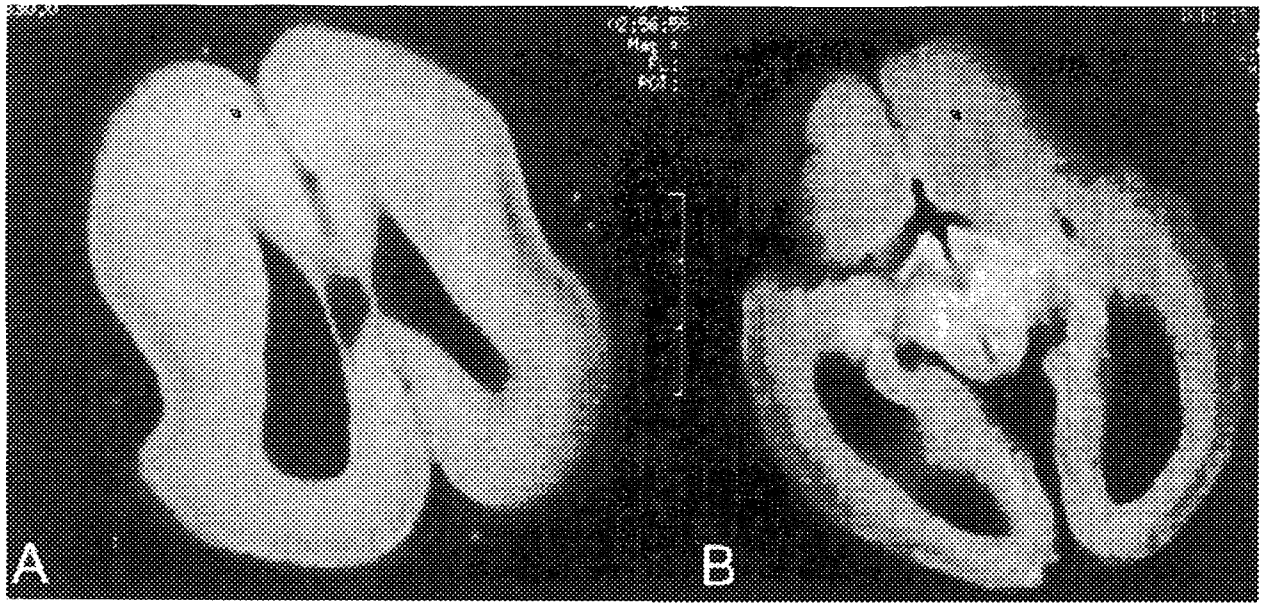

Figure 1. T_1-weighted magnetic resonance imaging brain scan (TR/TE = 8802/110 ms) depicting severe, grade 1 lissencephaly with diffuse agyria and no apparent gradient, and thick cortex. Interdigitations between the cortex and white matter were absent. (A) At the level of lateral ventricles: lateral ventricles were enlarged posteriorly. (B) At the level of midbrain: the opercula failed to fold over the insula.

A G-banding study of the patient's peripheral blood (Fig 2) revealed a 46,XX,add(17)(p13.1~13.3) karyotype: deletion of 17p13.1 to p13.3 and addition of extra chromosomal material of unknown origin. Her parents' peripheral blood karyotypes were normal. Fluorescence in situ hybridization studies of the patient's peripheral blood were ordered from a clinical molecular cytogenetic laboratory using commercially available probes: the 17p subtelomere probe (Vysis; Catalog number: 33-252017) and the LSI *LIS1* probe at 17p13.3 (Vysis; Catalog number: 32-190065). The subtelomere probe yielded a single signal, indicating a 17p terminal deletion (data not shown), whereas the *LIS1* probe yielded two signals, indicating the presence of two copies of the *LIS1* locus (Fig 3A). The latter finding contradicted our clinical impression that the patient had Miller-Dieker syndrome.

We hypothesized that small deletions might not be detectable by the LSI *LIS1* fluorescence in situ hybridization study probe (Vysis) because this probe hybridizes to a 110-kb region flanking the *LIS1* locus. A smaller-sized (5-kb) probe spanning *LIS1* intron 1 was therefore generated using long-range polymerase chain reaction (primer sequences and polymerase chain reaction conditions are available upon request). The *LIS1* intron 1 fluorescence in situ hybridization study probe yielded one signal, confirming a partial deletion of the *LIS1* locus (Fig 3B). Because the 5′ end of the *LIS1* locus resides on the telomeric end, we concluded that the patient had a terminal deletion spanning from the 17p terminus to the 5′ end of the *LIS1* locus (Fig 4).

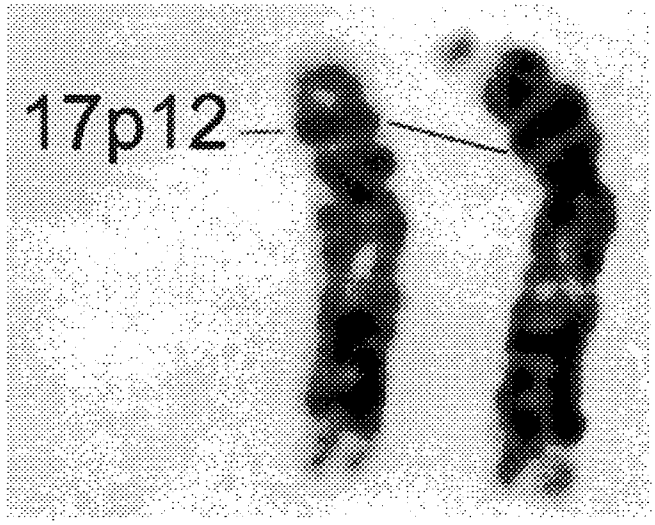

Figure 2. G-banded partial karyogram of the patient. Note deletion of 17p13.1 to p13.3 and addition of extra chromosomal material of unknown origin.

Discussion

This report describes a classic Miller-Dieker syndrome patient who received a false-negative result when a fluorescence in situ hybridization study was performed using a widely used commercial fluorescence in situ hybridization probe. Further studies using a "custom-made" probe resolved the apparent discrepancy between the clinical phenotype and the molecular cytogenetic test results.

The present case exemplifies a major shortcoming of commercially available fluorescence in situ hybridization studies for the diagnosis of microdeletion syndromes like Miller-Dieker syndrome: relatively small deletion can potentially remain undetected. Clinicians should be aware of this limitation of commercial fluorescence in situ hybridization study testing. When the clinical and laboratory results disagree, additional studies using smaller probes may be warranted. Any genetic region of interest can be amplified using long-range polymerase chain reaction and subsequently used as a fluorescence in situ hybridization study probe to search for small deletions, thanks to the availability of the complete human genome sequence.

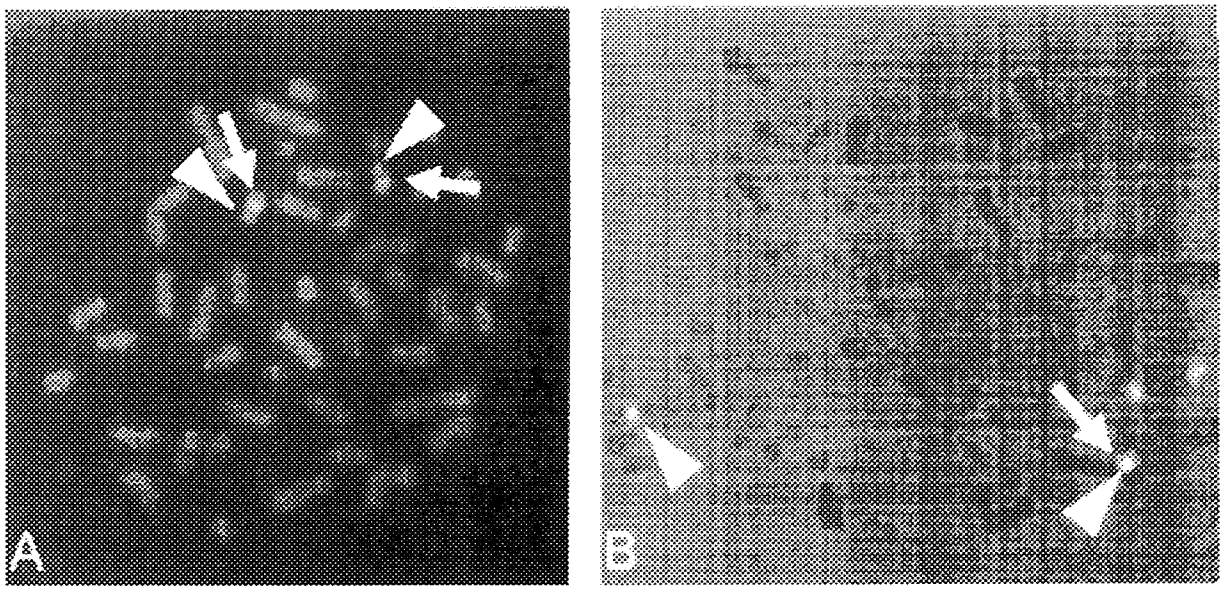

Figure 3. Fluorescence in situ hybridization analysis on metaphase spreads of the patient. (A) No detectable deletion of LIS1 when hybridized with LSI LIS1 Vysis probes (red signals, arrowheads) and LSI retinoic acid receptor alpha control probes (green signals, arrows). (B) Deletion in one of the chromosome 17 homologs when hybridized with digoxigenin-labeled polymerase chain reaction product containing LIS1 intron probes (red signal, arrow) and chromosome 17 centromere probes (green signals, arrowheads).

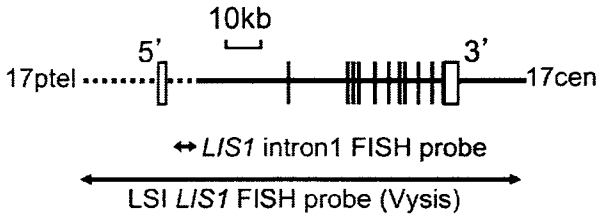

Figure 4. The presumed location of the deletion and the probes used for the fluorescence in situ hybridization studies. Dashed line indicates deleted region. Open boxes and closed boxes represent coding exons and untranslated regions.

Supported by a grant from The Ministry of Health, Labour, and Welfare of Japan.

References

[1] **Miller** JQ. Lissencephaly in two siblings. Neurology 1963:13: 841-50.

[2] **Dieker** H, Edwards RH. ZuRhein G, Chou SM. Hartman HA. Opitz JM. The lissencephaly syndrome. Birth Defects Orig Artic Ser 1969:5:53-64.

[3] **Jones** KL. Gilbert EF, Kaveggia EG, Opitz JM. The Miller-Dieker syndrome. Pediatrics 1980:66:277-81.

[4] **Reiner** O, Carrozzo R. Shen Y, et al. Isolation of a Miller-Dieker lissencephaly gene containing G protein beta-subunit-like repeats. Nature 1993:364:717-21.

[5] **Cardoso** C. Leventer RJ. Ward HL, et al. Refinement of a 400-kb critical region allows genotypic differentiation between isolated lissencephaly, Miller-Dieker syndrome, and other phenotypes secondary to deletions of 17p13.3. Am J Hum Genet 2003:72:918-30.

[6] **Ashwal** S. Congenital structural defects. In: Swaiman K, Ashwal S, Ferriero DM. Pediatric neurology, 4th ed. Philadelphia: Mosby Elsevier, 2006:413-7.

[7] **Kuwano** A. Ledbetter SA, Dobyns WB, Emanuel BS, Ledbetter DH. Detection of deletions and cryptic translocations in Miller-Dieker syndrome by in situ hybridization. Am J Hum Genet 1991:49:707-14.

[8] **Dobyns** WB. Truwit CL, Ross ME, et al. Differences in the gyral pattern distinguish chromosome 17-linked and X-linked lissencephaly. Neurology 1999:53:270-7.

American Journal of Medical Genetics Part A 143A:1815–1820 (2007)

Upper Airway Obstruction in Neonates and Infants With CHARGE Syndrome

Yoko Naito,[1] Masataka Higuchi,[2] Goro Koinuma,[1] Michihiko Aramaki,[1] Takao Takahashi,[1] and Kenjiro Kosaki[1]*

[1]Department of Pediatrics, Keio University School of Medicine, Tokyo, Japan
[2]Department of Pulmonology, National Center for Child Health and Development, Tokyo, Japan

Received 30 January 2007; Accepted 8 April 2007

Upper airway obstruction can be life-threatening in neonates and infants with CHARGE syndrome, many of whom undergo intratracheal intubation early in life. Although some of these patients are successfully extubated, others require tracheotomy. Deciding whether to complete tracheotomy is challenging since there are no clear criteria upon which to base this decision. We assessed 10 infants with CHARGE syndrome, 5 of whom required tracheotomy. Fiberoptic laryngoscopy showed that all of these patients shared certain features: anteroposterior flattening of the larynx; short vocal cords; anteriorly positioned, tall and hypertrophic arytenoids obscuring the glottis; uncoordinated movement of the vocal cords, epiglottis and arytenoids; salivary pooling. In addition, we observed only in those requiring tracheotomy an obstructive supraglottis that prevented visualization of the vocal cords throughout respiration. Salivary retention was much more severe in this group. These findings might be helpful for predicting the need for an early tracheotomy in situations where the vocal cords are not visible throughout the entire respiratory cycle. Given the high prevalence of malformed larynx and abnormal cranial nerve function, which are not alleviated by supraglottoplasty, we suggest that a thorough investigation of upper airway obstructive entities other than laryngomalacia be performed before embarking on supraglottoplasty in patients with CHARGE syndrome. © 2007 Wiley-Liss, Inc.

Key words: CHARGE syndrome; fiberoptic laryngoscopy; tracheotomy; cranial nerves; laryngomalacia

How to cite this article: Naito Y, Higuchi M, Koinuma G, Aramaki M, Takahashi T, Kosaki K. 2007. Upper airway obstruction in neonates and infants with CHARGE syndrome. Am J Med Genet Part A 143A:1815–1820.

INTRODUCTION

Hall first described [1979] and Pagon later coined the term CHARGE to represent a constellation of non-randomly associated malformations: C, coloboma of the iris or retina; H, heart defects; A, atresia of the choanae; R, retardation of growth and/or development; G, genital anomalies; and E, ear abnormalities [Pagon et al., 1981]. Numerous additional malformations that are not part of the acronym have also been frequently described in these patients, including those which involve the airway [Morgan et al., 1993; Roger et al., 1999; White et al., 2005]. Indeed, laryngomalacia, retrognathia, glossoptosis, intubation difficulties, esophageal fistula, laryngeal paralysis and clefts have often been reported [Asher et al., 1990; Stack and Wyse, 1991; Morgan et al., 1993; Aramaki et al., 2006].

A tracheotomy is performed in 10–60% of infants with CHARGE syndrome [Asher et al., 1990; Stack and Wyse, 1991; Morgan et al., 1993; Senders and Navarrete, 2001] who suffer from life-threatening upper airway obstructions after birth and require prolonged mechanical ventilation. Despite the high rate of tracheotomies performed on infants with CHARGE syndrome, precise descriptions of the laryngopharyngeal malformations or dysfunctions involved have been limited. Moreover, no reliable measures exist for predicting the natural course of the respiratory status in patients with CHARGE syndrome, and deciding whether to perform a tracheotomy in these patients is very demanding.

We expect that mechanisms underlying upper airway obstruction have a major impact on the natural course of the respiratory status of infants with CHARGE syndrome. Several mechanisms have been implicated in laryngopharyngeal dysfunction in CHARGE syndrome. Laryngomalacia is frequent

Grant sponsor: The Ministry of Health, Labour, and Welfare of Japan.
*Correspondence to: Kenjiro Kosaki, M.D., Department of Pediatrics, Keio University School of Medicine, 35 Shinanomachi, Shinjuku-ku, Tokyo 160-8582, Japan. E-mail: kkosaki@sc.itc.keio.ac.jp
DOI 10.1002/ajmg.a.31851

(8–37%) and is considered to be the major cause of upper airway obstruction in patients with CHARGE syndrome [Stack and Wyse, 1991; Morgan et al., 1993; White et al., 2005]. The underlying anatomical abnormality associated with laryngomalacia is a prolapse of the supraglottic tissues into the laryngeal lumen during inspiration; this abnormality may involve the epiglottis, aryepiglottic folds and the arytenoids. Although laryngomalacia usually resolves spontaneously by 2 years of age, it has been reported that 10–22% of the patients require surgery but usually have a good prognosis [Friedman et al., 1990; Loke et al., 2001]. However, the low success rate of supraglottoplasty in patients with CHARGE syndrome [Roger et al., 1999; Senders and Navarrete, 2001; Denoyelle et al., 2003; White et al., 2005] led us to consider that mechanisms other than laryngomalacia may also contribute to upper airway obstruction. Indeed, Roger et al. [1999] have described the condition of the larynx in patients with CHARGE syndrome as pharyngolaryngeal hypotonia, an upper airway obstructive entity that is distinct from laryngomalacia. They pointed out that supraglottic obstruction was present in these patients, despite the absence of the anatomical malformations found in laryngomalacia. The airway instability was ascribed to the incoordination of the hypotonic pharyngolarynx.

Alternatively, children with CHARGE syndrome are also likely to have cranial neuropathies [Byerly and Pauli, 1993]. Cranial nerves (CN) V, VII, VIII, IX and X are the most typically affected nerves in these patients [Lawland et al., 2003]. Of these, CN VII, IX and X neuropathies are associated with laryngeal discoordination and swallowing dysfunction [Arvedson and Lefton-Greif, 1996]. Aspiration is one of the most serious abnormalities of swallowing function. White et al. [2005] have reported that 20% of patients with CHARGE syndrome enrolled in their study demonstrated abnormal pharyngeal motility, saliva pooling, or laryngeal penetration and were considered to be at risk for aspiration. Gastroesophageal reflux is another comorbidity that is present in more than 80% of patients with CHARGE syndrome [Roger et al., 1999]. The high prevalence of gastroesophageal reflux may explain the particularly severe feeding intolerance and airway management complications in these patients.

In the present study, we performed comprehensive fiberoptic laryngoscopic examinations in 10 patients with CHARGE syndrome to delineate the laryngeal characteristics of patients with or without a tracheotomy.

PATIENTS AND METHODS

Ten consecutive patients with CHARGE syndrome who were referred to our Department between 2000 and 2006 underwent fiberoptic laryngoscopy using standard techniques as part of routine clinical care. Of these 10 patients, 5 underwent tracheotomy (Trach+ group) and 5 did not (Trach− group). The respiratory status of all patients was recorded and a Machida ENT 30PH pediatric model fiberoptic laryngoscope with a distal tip diameter of 3.2 mm was used. An Olympus XP40 pediatric model fiberoptic laryngoscope with a distal tip of 2.8 mm was used when suction was necessary to maintain the laryngeal view. The exams were performed by a single pediatric pulmonologist (M.H) while the patients were awake and in a supine position. Mandibular elevation or examination in the prone position was performed to obtain a view of the vocal cords, when necessary. The fiberoptic laryngosocpic examination was part of routine clinical care and so no local institutional review board involvement occurred.

The following observations were made: general appearance of the larynx; site of obstruction; anatomical abnormalities and mobility of the arytenoids, vocal cords, and epiglottis; glossoptosis; and the severity of saliva retention in the larynx. The severity of saliva pooling was determined by the frequency of suctioning necessary to maintain an adequate laryngeal view during the exam: mild, one to two times; moderate, more than three times; and severe, no adequate laryngeal view achieved despite continuous suctioning.

The clinical diagnoses of CHARGE syndrome were made based on the Blake criteria and were made by a single dysmorphologist (KK) [Blake et al., 1998]. Three of the 10 patients were screened for *CHD7* mutations and showed loss-of-function mutations, of which two were previously reported [Aramaki et al., 2006].

RESULTS

Respiratory and Feeding Status

Table I presents the clinical feature of the patients with CHARGE syndrome. The respiratory statuses of the patients from birth are summarized in Table II. Neonatal respiratory distress requiring early intratracheal intubation occurred in one Trach− patient and three Trach+ patients. Two patients, Patients 6 and 7, who did not require neonatal intubation eventually underwent ventilation support. Patient 6 failed to be extubated after endotracheal intubation for safety reasons while being transferred to our hospital, and Patient 7 failed to be extubated after a temporary intubation for a cardioangiogram. Of note, only one patient (Patient 3) had unilateral choanal atresia without any symptoms of upper airway obstruction. This patient did not undergo any surgical procedure to achieve better choanal patency. The laryngeal anomalies did not change or improve during the follow-up period

TABLE I. Clinical Features of the Patients

Patient	Trach	Sex	C	H	A	R	G	E	CND	Others
1	–	M	Yes	PDA	No	Yes	Yes	Yes	VII, VIII	CP, TEF
2	–	M	Yes	—	No	Yes	Yes	Yes	VIII	—
3	–	F	Yes	PDA, ASD	Yes	Yes	Not apparent	Yes	VIII	CL/P
4	–	M	Yes	DORV, VSD	No	Yes	Yes	Yes	VIII	—
5	–	F	Yes	ASD, VSD, PDA	No	Yes	Not apparent	Yes	VIII	—
6	+	M	Yes	DORV	No	Yes	Yes	Yes	VII, VIII	CL/P
7	+	M	Yes	—	No	Yes	Yes	Yes	VII, VIII	CL/P
8	+	M	Yes	Interruption of Ao	No	Yes	Yes	Yes	VII, VIII	CL/P
9	+	F	Yes	PDA	No	Yes	Yes	Yes	VII,VIII	—
10	+	M	Yes	TGA	No	Yes	Yes	Yes	VII, VIII	CL/P, TEF

C, coloboma; H, heart defect; A, choanal atresia; R, growth and mental retardation; G, hypoplastic genitalia; E, ear anomalies and hearing loss; CND, cranial nerve dysfunction; PDA, patent ductus arteriosus; DORV, double outlet right ventricle; ASD, atrial sepatal defect; CP, cleft palate; CL/P, cleft lips and palate; TEF, tracheoesophageal fistula.

(20 months–6 years, median of 4 years) in all the Trach+ patients.

The feeding statuses of the patients are summarized in Table II. Complete oral feeding was accomplished in three patients in the Trach– group. All the patients in the Trach+ group depended on nasogastric tube feeding. Two Trach– patients and all the Trach+ patients were clinically diagnosed as having gastroesophageal reflux (GER), of which two patients (Patients 6 and 10) required fundoplication procedures.

Laryngeal Structure

The fiberoptic laryngoscopic findings in the Trach– and Trach+ groups are summarized in Table III and actual photos are shown in Figures 1 and 2. In all the patients, the larynx exhibited an anteroposterior flattened appearance. Pharyngolaryngeal hypotonia was present in all the patients in both groups. In the Trach– group, the airway patency was not maintained during expiration. In the Trach+ group, the complete collapse of the laryngopharynx was observed throughout respiration. Laryngomalacia was observed in one patient in the Trach+ group (Patient 7). The laryngeal anomalies did not change or improve during the follow-up period (20 months–6 years, median of 4 years) in all the Trach+ patients.

Arytenoids

The arytenoids were anteriorly positioned, tall and hypertrophic. All the patients in the Trach– group presented with arytenoids that obscured the vocal cords only during expiration. Although limited, the functional movements of the arytenoids were conserved in this group, securing airway patency during inspiration. In the Trach+ group, the arytenoids, together with the epiglottis which came into contact with the posterior laryngeal wall, obscured the vocal cords throughout respiration. The arytenoids in this group lacked the ability to abduct.

Vocal Cords

Short and abducted vocal cords were seen in four Trach– (Patients 1, 2, 3 and 4) and all the Trach+ infants. In the Trach– group, the vocal cords were observable during inspiration; however, complete adduction could not be confirmed during expiration because of the anteriorly positioned arytenoids which obscured the vocal cords. In the Trach+ group, the vocal cords were completely obscured by

TABLE II. Patients' Respiratory and Feeding Statuses

Patient	Trach	Gestational age (weeks)	Birth weight (g)	NRD	Age at intubation (days)	Age at extubation (days)	Age at tracheotomy (m)	Feeding status
1	–	38	2,980	–	—	—	—	Oral, GER
2	–	38	3,420	–	—	—	—	Oral
3	–	37	2,360	–	—	—	—	NG-tube, GER
4	–	40	3,440	+	1	3	—	Oral
5	–	40	2,705	–	—	—	—	Oral and G-tube
6	+	41	3,084	–	35	Failed	3	NG-tube, GER, fundoplication
7	+	41	3,056	–	33	Failed	2	NG-tube, GER
8	+	41	3,374	+	3	Failed	4	NG-tube, GER
9	+	40	2,750	+	3	Failed	9	NG-tube, GER
10	+	41	2,850	+	1	Failed	4	NG-tube, GER, fundoplication

NRD, neonatal respiratory distress; GER, gastroesophageal reflux; NG-tube, nasogastric tube.

TABLE III. Fiberoptic Laryngoscopic Findings of Trach− and Trach+ Groups

	Trach− group (n = 5)	Trach+ group (n=5)
Laryngeal structure		
Anteroposterior flattened appearance	5	5
Pharyngolaryngeal hypotonia		
Inspiration	0	5
Expiration	5	5
Laryngomalacia	0	1
Arytenoids		
Malformation (tall and hypertrophic)	5	5
Mobility		
Adduction (incomplete or impaired)	0	5 (all fixed at adducted position)
Abduction (incomplete or impaired)	5 (incomplete)	5 (impaired)
Vocal cords		
Malformation (short)	4	5
Visualization		
Visible during inspiration	5	0
Visible during expiration	0	0
Mobility		
Adduction (incomplete or impaired)	5 (incomplete)	5 (impaired)
Abduction (incomplete or impaired)	0	5 (all fixed at abducted position)
Epiglottis		
Malformation		
Length-wise folding (laryngomalacia)	0	1
Mobility		
Posterior laryngeal wall contact	0	5
Glossoptosis	5	5
Saliva retention		
Mild	1	
Moderate	1	
Severe		5

the arytenoids throughout respiration and could be visualized only when the laryngoscope was advanced beyond the arytenoids. The cords were in an abducted position, and lacked the ability to adduct.

Epiglottis and Glossoptosis

In all the patients in the Trach+ group, the epiglottis was in intermittent contact with the posterior laryngeal wall throughout respiration and, together with the arytenoids, obscured the vocal cords. Mild laryngomalacia characterized by a slight length-wise folding of the epiglottis during inspiration was observed in Patient 7. Glossoptosis that could not be improved by adequate mandibular elevation or by positioning the patient in a prone position was observed in all the Trach+ patients.

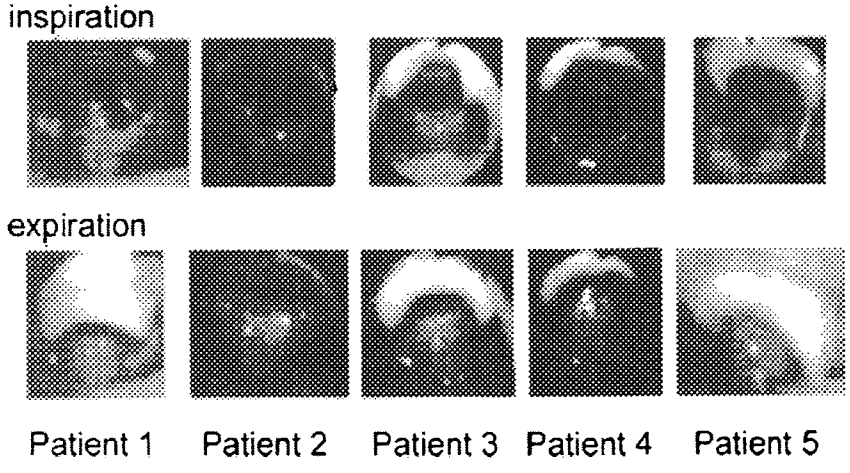

FIG. 1. Fiberoptic laryngoscopic views of the Trach− group (top row: inspiration views, bottom row: expiration views). Short vocal cords are visible during inspiration. During expiration, the arytenoids and epiglottis obscure the vocal cords. The arytenoids are anteriorly positioned, tall and hypertrophic.

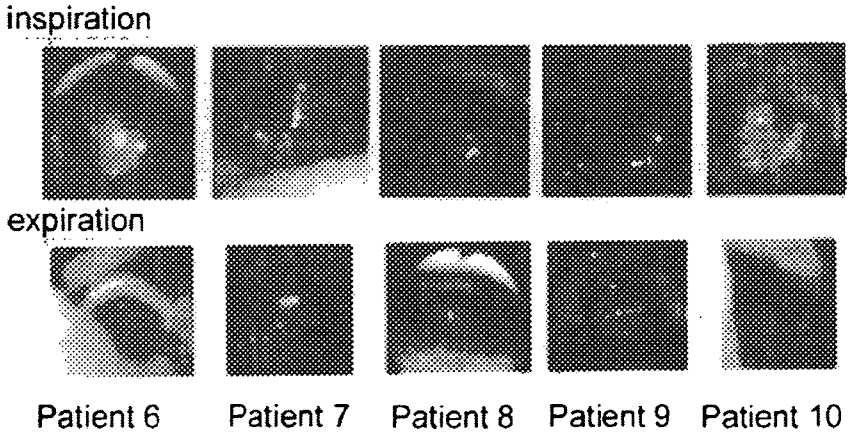

FIG. 2. Fiberoptic laryngoscopic views of the Trach+ group (top row: inspiration views, bottom row: expiration views). Vocal cords are completely obscured by the arytenoids and epiglottis throughout respiration. The arytenoids are anteriorly positioned, tall and hypertrophic.

Saliva Retention and Cranial Nerve Dysfunction

Two Trach− patients (Patients 1 and 3) had mild and moderate saliva retention, respectively. All the Trach+ patients had severe saliva retention. One Trach− patient (Patient 1) and all the Trach+ patients had apparent facial palsy. Cranial nerve VIII dysfunction was seen in all the patients.

DISCUSSION

All patients in our study had upper airway obstruction at the level of the larynx. Although the severity and the timing of the obstruction varied between the Trach− and Trach+ groups, a hypotonic larynx with hypertrophic arytenoids and uncoordinated movement of the supraglottis were the major factors making airway patency difficult to maintain. In contrast to the airways in the Trach− group, which were obstructed during expiration, continuous obstruction was observed in the Trach+ group.

Distinctive differences were present between the two groups: first, the vocal cords of the Trach− group could be visualized during inspiration, whereas the cords of the Trach+ group were completely obscured by the arytenoids and epiglottis throughout respiration. Second, the mobility of the arytenoids, vocal cords and epiglottis was impaired in the Trach+ group throughout respiration. The arytenoids did not abduct during inspiration and, together with the discoordinate movement of the epiglottis, they obstructed the glottis. The vocal cords were fixed in the abducted position throughout respiration, allowing secretions to drain into the airway. Third, severe saliva pooling was found only in the Trach+ group. Although Patients 3, 4, 5, 6, 8, 9 and 10 had undergone cardiac operations that may have involved the mobilization of the recurrent laryngeal nerve, thereby inducing the impaired dynamics of the larynx including the swallowing dysfunction, the features observed in our study may be congenital, since malformed and discoordinate larynx with severe saliva pooling was observed on the day of birth in both Patients 8 and 10, prior to their cardiac operations. Laryngeal characteristics seen only in the Trach+ group were observed during fiberoptic laryngoscopy examinations performed prior to the tracheotomies; thus the differences observed between the Trach+ and Trach− groups were not caused by the placement of the tracheostomy. Furthermore, the laryngeal anomalies did not change or improve during the follow-up period in all the Trach+ patients.

Previous studies have indicated that cranial nerve dysfunction is an aggravating factor in upper airway obstruction of patients with CHARGE syndrome [Senders and Navarrete, 2001; Denoyelle et al., 2003]. We emphasize the frequent occurrence of cranial nerve involvement: first, severe saliva retention was common among the Trach+ group in our study (5/5). Saliva retention can be ascribed to a swallowing intolerance associated with the poor coordination of the pharyngolaryngeal muscles [Arvedson and Lefton-Greif, 1996] due to impairment of CNs VII, IX and X [Dobbelsteyn et al., 2005]. Byerly and Pauli [1993] have reported that 31% of the reviewed cases with CHARGE syndrome had clinical signs and/or symptoms of possible CN IX and/or X dysfunction. They also suggested that the feeding difficulties seen in CHARGE syndrome may be due primarily to dysfunction of CNs IX and X. Second, GER was prevalent (5/5) among the Trach+ group. The major mechanism for GER is transient lower esophageal sphincter relaxation [Kalia and Mesulam, 1980; Blackshaw et al., 1987; Mittal et al., 1995], which is mediated via the vagal pathway [Holloway et al., 1989; Staunton et al., 2000; Martin et al., 2002]. Thus, neuromuscular incoordination of the larynx

and severity of saliva pooling in association with GER may worsen the respiratory status of these patients.

Typically, supraglottoplasty has been attempted in many patients with CHARGE syndrome, based on the premise that laryngomalacia is the major factor contributing to upper airway obstruction in these patients [Morgan et al., 1993; White et al., 2005]. However, most of the reported cases had poor outcomes [White et al., 2005] or even suffered from major complications, such as supraglottic stenosis [Roger et al., 1999; Senders and Navarrete, 2001; Denoyelle et al., 2003; White et al., 2005]. In our study, only one Trach+ patient had mild laryngomalacia. The low success rate of supraglottoplasty suggests that, laryngomalacia, although frequently observed in patients with CHARGE syndrome, may not be the sole factor responsible for respiratory distress. Given the frequent occurrence of malformed larynx and abnormal cranial nerve function, which are not alleviated by supraglottoplasty, we suggest that a thorough investigation of upper airway obstructive entities other than laryngomalacia be performed before embarking on supraglottoplasty in patients with CHARGE syndrome.

We further suggest that an early tracheotomy may be helpful when the vocal cords are not visible throughout respiration and copious saliva pooling is present in the larynx. These features were only observed among patients with CHARGE syndrome who underwent tracheotomy and did not improve, either structurally or functionally, during the follow-up period. Although tracheotomy can cause non-negligible morbidity and mortality [Gianoli et al., 1990], especially when performed early and used for long periods, we prefer this option to waiting for further hypoxic events that could aggravate the developmental delays that are already disturbed in patients with CHARGE syndrome. However, this suggestion is based on our retrospective findings and needs to be validated in a larger prospective study.

REFERENCES

Aramaki M, Udaka T, Kosaki R, Makita Y, Okamoto N, Yoshihashi H, Oki H, Nanao K, Moriyama N, Oku S, Hasegawa T, Takahashi T, Fukushima Y, Kawame H, Kosaki K. 2006. Phenotypic spectrum of CHARGE syndrome with CHD7 mutations. J Pediatr 148:410–414.

Arvedson JC, Lefton-Greif MA. 1996. Anatomy, physiology, and development of feeding. Semin Speech Lang 17:261–268.

Asher BF, McGill TJ, Kaplan L, Friedman EM, Healy GB. 1990. Airway complications in CHARGE association. Arch Otolaryngol Head Neck Surg 116:594–595.

Blackshaw LA, Grundy D, Scratcherd T. 1987. Vagal afferent discharge from gastric mechanoreceptors during contraction and relaxation of the ferret corpus. J Auton Nerv Syst 18: 19–24.

Blake KD, Davenport SL, Hall BD, Hefner MA, Pagon RA, Williams MS, Lin AE, Graham JM Jr. 1998. CHARGE association: An update and review for the primary pediatrician. Clin Pediatr (Phila) 37:159–173.

Byerly KA, Pauli RM. 1993. Cranial nerve abnormalities in CHARGE association. Am J Med Genet 45:751–757.

Denoyelle F, Mondain M, Gresillon N, Roger G, Chaudre F, Garabedian EN. 2003. Failures and complications of supraglottoplasty in children. Arch Otolaryngol Head Neck Surg 129:1077–1080; discussion 1080.

Dobbelsteyn C, Marche DM, Blake K, Rashid M. 2005. Early oral sensory experiences and feeding development in children with CHARGE syndrome: A report of five cases. Dysphagia 20:89–100.

Friedman EM, Vastola AP, McGill TJ, Healy GB. 1990. Chronic pediatric stridor: Etiology and outcome. Laryngoscope 100: 277–280.

Gianoli GJ, Miller RH, Guarisco JL. 1990. Tracheotomy in the first year of life. Ann Otol Rhinol Laryngol 99:896–901.

Hall BD. 1979. Choanal atresia and associated multiple anomalies. J Pediatr 95:395–398.

Holloway RH, Wyman JB, Dent J. 1989. Failure of transient lower oesophageal sphincter relaxation in response to gastric distension in patients with achalasia: Evidence for neural mediation of transient lower oesophageal sphincter relaxations. Gut 30:762–767.

Kalia M, Mesulam MM. 1980. Brain stem projections of sensory and motor components of the vagus complex in the cat. II. Laryngeal, tracheobronchial, pulmonary, cardiac, and gastrointestinal branches. J Comp Neurol 193:467–508.

Lawland CMD, Blake KD, Prasad C, Graham JM Jr. 2003. The cranial nerve anomalies of CHARGE association/syndrome (A/S). Pediatr Child Health 8:26B.

Loke D, Ghosh S, Panarese A, Bull PD. 2001. Endoscopic division of the ary-epiglottic folds in severe laryngomalacia. Int J Pediatr Otorhinolaryngol 60:59–63.

Martin DM, Probst FJ, Fox SE, Schimmenti LA, Semina EV, Hefner MA, Belmont JW, Camper SA. 2002. Exclusion of PITX2 mutations as a major cause of CHARGE association. Am J Med Genet 111:27–30.

Mittal RK, Holloway RH, Penagini R, Blackshaw LA, Dent J. 1995. Transient lower esophageal sphincter relaxation. Gastroenterology 109:601–610.

Morgan D, Bailey M, Phelps P, Bellman S, Grace A, Wyse R. 1993. Ear–nose–throat abnormalities in the CHARGE association. Arch Otolaryngol Head Neck Surg 119:49–54.

Pagon RA, Graham JM Jr, Zonana J, Yong SL. 1981. Coloboma, congenital heart disease, and choanal atresia with multiple anomalies: CHARGE association. J Pediatr 99:223–227.

Roger G, Morisseau-Durand MP, Van Den Abbeele T, Nicollas R, Triglia JM, Narcy P, Abadie V, Manac'h Y, Garabedian EN. 1999. The CHARGE association: The role of tracheotomy. Arch Otolaryngol Head Neck Surg 125:33–38.

Senders CW, Navarrete EG. 2001. Laser supraglottoplasty for laryngomalacia: Are specific anatomical defects more influential than associated anomalies on outcome? Int J Pediatr Otorhinolaryngol 57:235–244.

Stack CG, Wyse RK. 1991. Incidence and management of airway problems in the CHARGE association. Anaesthesia 46:582–585.

Staunton E, Smid SD, Dent J, Blackshaw LA. 2000. Triggering of transient LES relaxations in ferrets: Role of sympathetic pathways and effects of baclofen. Am J Physiol Gastrointest Liver Physiol 279:G157–162.

White DR, Giambra BK, Hopkin RJ, Daines CL, Rutter MJ. 2005. Aspiration in children with CHARGE syndrome. Int J Pediatr Otorhinolaryngol 69:1205–1209.

GENETIC TESTING
Volume 11, Number 3, 2007

DOI: 10.1089/gte.2006.0519

Screening for Alagille Syndrome Mutations in the *JAG1* and *NOTCH2* Genes Using Denaturing High-performance Liquid Chromatography

HAZUKI SAMEJIMA,[1] CHIHARU TORII,[1] RIKA KOSAKI,[2] KENJI KUROSAWA,[3] HIROSHI YOSHIHASHI,[3] KOJI MUROYA,[4] NOBUHIKO OKAMOTO,[5] YORIKO WATANABE,[6] TOMOKI KOSHO,[7] MICHIRU KUBOTA,[8] OSAMU MATSUDA,[9] MIWA GOTO,[1] KOSUKE IZUMI,[1] TAKAO TAKAHASHI,[1] and KENJIRO KOSAKI[1]

ABSTRACT

Mutations in the *JAG1* gene and the *NOTCH2* gene cause Alagille syndrome. At present, however, genetic testing of Alagille syndrome is not commonly applied in clinical settings because the currently available assays are technically and financially demanding, mainly because of the size of the genes. In the present study, we optimized the highly sensitive and specific mutation scanning method automated denaturing high-performance liquid chromatography (DHPLC) to analyze the entire coding region of *JAG1* and *NOTCH2*. The coding region was amplified by 69 primer pairs, all of which have the same cycling conditions, aliquoted on a 96-well format PCR plate. In this manner, all the exons were simultaneously amplified using a single block in a thermal cycler. We then wrote a computer script to analyze each segment of *JAG1* and *NOTCH2* by DHPLC in a serial manner using conditions that were optimized for each amplicon. The implementation of this screening method for *JAG1* and *NOTCH2* will help medical geneticists confirm their clinical impressions and provide accurate genetic counseling to the patients with Alagille syndrome and their families.

INTRODUCTION

ALAGILLE SYNDROME (MIM 118450) represents an autosomal dominant condition characterized by a constellation of malformations: a paucity of intrahepatic bile ducts, posterior embryotoxon, and retinal pigmentary changes in the eye, pulmonic valvular stenosis and peripheral arterial stenosis in the heart; abnormal vertebrae ("butterfly" vertebrae), and decrease in interpediculate distance in the lumbar spine in the skeletal system; broad forehead, pointed mandible, and bulbous tip of the nose (Watson and Miller 1973;Alagille *et al.* 1975), and renal dysplasia (LaBrecque *et al.* 1982).

Mutations in the *Jagged 1* gene (*JAG1*) on chromosome 20p11.2 were identified as causative of this syndrome in 1997 (Li *et al.* 1997; Oda *et al.* 1997). *JAG1* encodes a transmembrane protein acting as ligand for the evolutionarily conserved Notch signaling pathway. Since then, more than 24 mutation analyses have been published regarding this locus. In 2006, *NOTCH2*, a notch signaling receptor, was identified as the second causative gene for Alagille syndrome (McDaniell *et al.* 2006). Among 11 *JAG1* mutation-negative probands, two probands with Alagille syndrome were identified as having *NOTCH2* mutations. The 11 patients derived from 247 Alagille probands. Hence, only a small fraction (*i.e.*, 2/247) of patients with Alagille syndrome had *NOTCH2* mutations.

AU1 [1]Department of Pediatrics, Keio University School of Medicine, [2]Department of Clinical Genetics and Molecular Medicine, National Children's Medical Center, Divisions of [3]Medical Genetics and [4]Endocrinology, Kanagawa Children's Medical Center, Tokyo, Japan.
[5]Department of Planning and Research, Osaka Medical Center and Research Institute for Maternal and Child Health, [6]Department of Pediatrics and Child Health, Kurume University School of Medicine.
[7]Department of Medical Genetics, Shinshu University School of Medicine.
[8]Department of Pediatrics, Hokkaido University School of Medicine.
[9]Department of Pediatrics, Ehime University School of Medicine.

Alagille syndrome is characterized by extreme degree of variable expressivity and many atypical or mild cases have been reported (Kamath *et al.* 2003). Clinical diagnosis can be difficult in these cases, and sometimes liver biopsy is performed to search for paucity of intrahepatic bile duct, and molecular diagnosis represents a noninvasive alternative option to liver biopsy. Usefulness of the genetic test is exemplified in cases in which liver or kidney transplantation is undertaken. When severe hepatic (Kasahara *et al.* 2003) or renal failure (Schonck *et al.* 1998) occur in an Alagille syndrome patient, liver or kidney transplantation is performed. Occasionally, a graft is obtained from a living related donor (Kasahara *et al.* 2003), typically from either of the parents. As stated above, because of extreme degree of variable expressivity, potential donors can exhibit minimal clinical phenotype yet carries the same mutation as the patient (*i.e.*, the recipient). In order to prevent those asymptomatic carriers from being donors, liver biopsy may be performed. Molecular diagnosis can alleviate such invasive tests. At present, however, genetic testing of *JAG1* is not commonly applied in clinical settings because the currently available assays are technically and financially demanding, mainly because of the size of the *JAG1* gene, which comprises a coding sequence of 3657 bp in 26 exons. Since mutations in the second causative gene *NOTCH2* cause comparable phenotype, *NOTCH2*, which comprises a coding sequence of 7416 bp in 34 exons, needs to be screened for when no mutation is identified in *JAG1*. This requirement further increases the number of exons to be screened.

Generally speaking, two approaches can be taken when performing genetic testing in clinical settings. Most intuitively, all the coding exons can be amplified by PCR and then sequenced in parallel. Alternatively, screening procedures can be performed prior to the sequencing analysis to identify exon(s) that may harbor mutations. When the size of the gene (*i.e.*, the number of exons) is small, the first approach is more efficient. However, as the size of the gene increases, the second approach becomes more efficient from the standpoints of supply costs and labor. Because the human *JAG1* gene and the *NOTCH2* gene are relatively large, consisting of 60 exons altogether, clinical genetic testing of Alagille syndrome is best accomplished by the second method. Heritage *et al.* (2002) demonstrated that denaturing high-performance liquid chromatography (DHPLC) technique (O'Donovan *et al.* 1998; Wagner *et al.* 1999; Udaka *et al.* 2005b) is suitable for such screening. In the present study, we developed DHPLC-based systematic mutation screening system for semiautomated analysis of multiple exons of *JAG1* and *NOTCH2* (Kosaki *et al.* 2005), which requires minimal human intervention, with a consequent significant reduction of the labor cost (Aramaki *et al.* 2006). This article presents in detail the methods we have developed for finding mutations in the *JAG1* and *NOTCH2* genes, which cause the majority of cases of the Alagille syndrome.

MATERIALS AND METHODS

Patients and DNA preparation

Eighteen Japanese probands who had been clinically diagnosed as having Alagille syndrome (Alagille *et al.* 1987) were included in the study. All the patients *except for two* were simplex (*i.e.*, a single occurrence in a family). In families with multiple affected family members, only the probands were included. Each patient and family members were enrolled in the study after receiving their written informed consent, according to a protocol approved by an institutional review board. Genomic DNA was isolated using the QIAamp system (Qiagen Inc., Valencia, CA).

PCR amplification of the genomic DNA

The entire *JAG1* coding region (exons 1–26; GenBank sequence accession number NM_000214) was screened for mutations. We carefully selected the primer pairs to ensure that all of the primers could use the same cycling conditions. The primer pairs were designed to amplify the exons, exon–intron boundaries and at least 20 base pairs of the flanking intron sequences. Twelve of the 60 primers had been used in a previously published study (Oda *et al.* 1997). The remaining 48 (60–12) primers were designed by us. The optimized primer sequences are listed in Table 1.

PCR was performed in a volume of 20 μl containing 30 ng of genomic DNA, 10 pmol each of the forward and reverse primers, 0.2 m*M* of each dNTP, 2 m*M* $MgSO_4$, 0.5 units of Platinum *Taq* DNA polymerase High Fidelity (Invitrogen, Carlsbad, CA), and the buffer supplied by the manufacturer. Thermal cycling was done using a touchdown PCR protocol (Don *et al.* 1991); The annealing temperature was decreased by 0.5°C every second cycle beginning at 65°C and decreasing to a "touchdown" annealing temperature of 60°C, which was then used for 30 cycles.

JAG1 *mutation analysis*

PCR amplicons from human genomic DNA were analyzed by DHPLC according to the method developed by Oefner and Underhill (O'Donovan *et al.* 1998; Wagner *et al.* 1999; Udaka *et al.* 2005a) using an analysis system purchased from Transgenomic (Omaha, NE). To generate heteroduplexes, the PCR products were denatured at 95°C for 5 min and reannealed by cooling to 25°C with a temperature change of −1.5°C/min. After heteroduplex formation, the PCR amplicons were applied to a preheated reversed-phase column. An elution gradient was generated by mixing buffer A (0.1 mol/l triethylammonium acetate) and buffer B (0.1 mol/l triethylammonium acetate containing 250 ml/l acetonitrile) in a linear gradient from start to a final %B over a period of 4.5 min, as described in Table 1. Standard operating procedures for the instrument's operation and maintenance and for mutation detection by DHPLC (http://cmgs.org/bpg/Guidelines/2002/dhplc.htm) have been described (Schollen *et al.* 2005).

All DHPLC conditions, including the melting temperatures and buffer gradients specific to each PCR amplicon, were determined using melting temperature prediction software (Transgenomic WAVEMAKER). Multiple column temperatures were used when the software predicted that the fragment being analyzed consists of two or three different melting temperature domains. In that case, two or three analysis temperatures were needed to scan the entire exon sequence. Two or three temperature conditions were used for each amplicon, except for exons 2a, 2b, 3, 4b, 14, 17, 18, 19, 22, and 26c, which

TABLE 1. PCR PRIMER SEQUENCES AND DHPLC ANALYSIS CONDITIONS (TEMPERATURE AND GRADIENT) FOR *JAG1* MUTATION SCREENING

Exon[a]	*F/R*[b]	*Primer sequence (5'-3')*	*DHPLC temp (°C)*	*DHPLC gradient*[c] *(% B/4.5 min)*
1	F	TCCAATCGGCGGAGTATATTAGAGC[d]	66.2	52–61
	R	AGGACGGCTGGGAGGGA[d]	70.5	47–56
2a	F	GCTGACCTACCTCCTTCCCT	64.6	54–63
	R	GATGCGGTTGCGGTCGTTG		
2b	F	TCATCGGGGGCAACACCTTC	66.7	46–55
	R	CAGGCGCGGGTGTGAG		
3	F	TGACAAAGGAAGGGGAGTTGGTTTG	59.4	51–60
	R	GTTTAGAGAAAAGTCCACAGAAGCGATAC		
4a	F	TCAGGGAAGAAGGCTGCAATGTGAATA	57.6	51–60
	R	CTGGGGCGGCAGAACTTATTG[d]	63.6	45–54
4b	F	GCGTTGCCCQACTTTGAGTAT	60.9	52–61
	R	TGGTGGGGTGATAAATGGAC		
5	F	GCGTCCCGATGCAAGGAACAGGCAGTGT	57.2	53–62
	R	AGAAGTGGTGTGTGCATTCC	60.1	50–59
6	F	CAAAAGGCTAACCTGGAGGTGTG	62.7	50–59
	R	GATCCCACCCTGGGTCTCAT	63.7	49–58
7	F	TGGGTTCGCCATCTTCACAGG[d]	58.9	52–61
	R	CGAATCAGCATCACCCAAAAAACTTTAGAGA	60.0	51–60
8	F	ATCCCTCTCTGCTGCCATCC	60.4	51–60
	R	CTCTCCCCAGCTGGTATCTT	62.7	49–58
9	F	GGCCCGCCGCCCCCGCCGGTCAACCCCCTCCTTTTCTT	59.8	51–60
	R	CAATCAAAGCCAACCTTGGT6A	61.5	50–59
10	F	ATTTCTCATGCTCATCCCCATCTCCTT	58.6	50–59
	R	CAGCAAGTCGGCTACCCAAGTTT[d]	60.6	48–57
11	F	CCCAATTTCACTGTAAATTACCTCTTTAAAATGATGAC	53.3	49–58
	R	AGCTCTCCTAGTGTCGCACAAATCT		
12	F	CTGAAGCCCTGTGTTTGTGGAATAC	58.8	55–64
	R	GAAAAGTAAAGGGAAGCGGAGGAG[d]	60.5	53–62
13	F	CCCTCCCCCTTTTCGCTGTT[d]	60.2	52–61
	R	TAGTAAGTGGGGACAAAAGGAGCAAGT	62.7	50–59
14	F	GAATGCCGCATCTGTGGGTG[d]	61.2	53–62
	R	GCTGGGGAGCACTGGTC		
15	F	AGGAGGGAGCCATGAAAACTGC[d]	58.1	52–61
	R	AACATGACCCATACATCCCAGAG	61.3	49–58
16	F	GTGAATGGTCCTGGATCTCGTCTT[d]	59.8	52–61
	R	CCCTCCCACAGAAGACAGAG	63.0	48–57
17	F	GCTATCTCTGGGACCCTTCC	61.4	54–63
	R	CCAGGCCCAGAGAAATATCA		
18	F	TTATGATATTTCTCTGGGCCTGGTTCTTG	62.8	51–60
	R	CGACAGCCCTGGGAGAGTT		

TABLE 1. PCR PRIMER SEQUENCES AND DHPLC ANALYSIS CONDITIONS (TEMPERATURE AND GRADIENT) FOR *JAG1* MUTATION SCREENING (CONT'D)

Exon[a]	*F/R*[b]	*Primer sequence (5'-3')*	*DHPLC temp (°C)*	*DHPLC gradient*[c] *(% B/4.5 min)*
19	F	GCCTGGTTCCAATTTAGCAA	59.7	49–58
	R	GCGTCCCGCACGATAGTGGATGAGTGCTG		
20	F	AGAGTAATGGACTGGGAGGTTGGTAA[d]	60.3	50–59
	R	TGAGGCATGGAATGAAGCGGTAAAG	63.5	46–55
21	F	ACCATCAGTCCCTAAACTTGAACTCCATT	59.4	50–59
	R	GCTCACCCCAGAAGACCCAT	63.0	47–56
22	F	CAAAGGGCACAGGCATAACCATTTCATAA	61.1	51–60
	R	GTGAACTGCGGCAGCCATCAT	57.0	56–65
23	F	TTCTGGAATCAGGGATGAGC	61.0	52–61
	R	GCAGACATCCACCATTCAAA	64.5	48–57
24	F	CTCTCAATCTTACACGTGTGTGGGTTT	57.3	51–60
	R	CATCGAATAATGAGGTGTGAATGGGTC	60.3	48–57
25	F	TCGAGTAATTTTGAAGAAAGGCTGCTTTGAGTAT	57.9	53–62
	R	ATAATCCCTCGACCTGATGGCTTTATTGAA	59.9	51–60
26a	F	TTCTTTCTTTCTTGGAGAGTTAATTGGTTTTGTGC	60.3	53–62
	R	ATAATCCTTGATGGGGACCGTGTTG	64.4	49–58
26b	F	CAGCTGAACCAGATCAAAAACCCCA	58.7	52–61
	R	TGTTTGTCCAGTTTGGGTGTTTTGTCG	62.9	48–57
26c	F	GTACACGCTGGTAGACAGAGAAGA	61.9	50–59
	R	GACAGTTTAAAGAACTACAAGCCCTCAGA[d]		

[a]Some exons are amplified in multiple PCRs, designated a, b, etc., and some PCRs contain more than one exon.
[b]F, upstream primer; R, downstream primer.
[c]Buffer A is 0.1 *M* triethylammonium acetate; Buffer B is 0.1 *M* triethylammonium acetate containing 25% (v/v) acetonitrile. "52–61" indicates that the gradient consists of 52% B: 48% A through to 61% B: 39% A.
[d]Primers which had been used in a previously published study (Oda *et al.*, 1997).

were subjected to only a single condition. The optimized DHPLC conditions for each amplicon are listed in Table 1.

When the chromatographic analyses of all the amplicons were completed, the DHPLC profiles were visually compared with the profiles of normal controls. PCR products corresponding to all variant elution profiles of the DHPLC were purified using a desalting column and were sequenced bidirectionally using the dideoxy sequencing method (BigDye Dideoxy sequencing kit; Applied BioSystems, Foster City, CA) and an automated sequencer (ABI3100; Applied Biosystems). The sequence-verification primers were the same as the PCR primers.

NOTCH2 *mutation analysis*

We analyzed the entire coding region (exons 1–34) of the *NOTCH2* gene in five genetic samples from patients in whom no *JAG1* mutations had been identified. The entire *NOTCH2* coding region (exons 1–34; GenBank sequence accession number NM_024408) was screened for mutations. We carefully selected the primer pairs to ensure that all of the primers could use the same cycling conditions. All the primer pairs except for one (McDaniell *et al.* 2006) were designed by us. The optimized primer sequences are listed in Table 2. All DHPLC conditions, including the melting temperatures and buffer gradients specific to each PCR amplicon, were determined using melting temperature prediction software (Transgenomic WAVEMAKER) and optimized as described above. Two to four temperature conditions were used for each amplicon, except for exons 1, 2, 10, and 22, which were subjected to only a single condition. The optimized DHPLC conditions for each amplicon are listed in Table 2.

Site-directed mutagenesis of NOTCH2

In order to confirm that our method is adequate for the detection of *NOTCH2* mutations, we generated PCR amplicons containing all previously described mutant alleles of *NOTCH2*, 1331G>A(C444Y), and IVS32-1G>A , using the "splicing by overlap extension" (SOE) PCR method (Horton *et al.* 1990.

TABLE 2. PCR PRIMER SEQUENCES AND DHPLC ANALYSIS CONDITIONS (TEMPERATURE AND GRADIENT) FOR *NOTCH2* MUTATION SCREENING

Exon[a]	*F/R*[b]	*Primer sequence (5'-3')*	*DHPLC temp (°C)*	*DHPLC gradient*[c] *(% B/4.5 min)*
1	F	CACACGAGGCTGCTTCGT[d]	68.0	56–65
	R	CACACGAGGCTGCTTCGT[d]		
2	F	CTAAAACACAGGAAATAAGAGCATC	56.5	58–67
	R	TCTTATTAGCCAATTATCTGGCATC	58.5	55–64
3	F	TGTTTTCATGGACTCTTCTCTTTTC	61.5	53–62
	R	GGTATCTGCTGAAGGTAGGAAAC	64.0	50–59
4	F	CTATTTCTGTGGCCAGTACTGAGTT	60.8	58–67
	R	CTCACTTCCCTTTTTCCTTGG	62.8	56–65
5	F	CAGGTCGTTTCTTCTGTATGAGATT	59.5	51–60
	R	GCAGGCCTAAGATATTTGTTACTGA	61.2	49–58
6	F	GCTGGTATGGTACTAGTCCTTTGAG	59.6	55–64
	R	CCTGTTTCTAGATCCGTCCTTCTG	62.3	53–62
7	F	GAAGTTGCGTATAAATCTCCATGTT	59.4	56–65
	R	GGAATATATGGTTATGGCTATGCTG	60.8	53–62
8	F	ATGCTATAACCATCAGATGCTCTTC	58.4	55–64
	R	GAATGCTCTACCAAGAGAAGTTCAG	60.2	53–62
			61.0	53–62
9	F	TTCTCTCTCTTTAAGCCACTTGTGT	57.2	53–62
	R	TACTCTAATGATTTCCTCATGCACA	60.2	50–59
			61.3	49–58
10	F	CCTAACATCATTCTCATGGTAAAGG	59.5	54–63
	R	AGAAACAGCTCTTCCTAAACACAGA		
11	F	CTTGGTCTTTGAGAATCCTTGATAA	58.5	55–64
	R	ACAGATTTGAGAAACAGTGAAAACC	61.1	52–61
			62.3	51–60
12	F	CATCACAAGCAGAAAGCCTTAGTAT	57.4	52–61
	R	GAAATAGGAAACACTTGAQAAAGCAA	60.1	51–60
13	F	AGTTCTGGGTCTATTTCCTAAGCAT	60.2	53–62
	R	AACTGGCTTAACACAGGTCAATAAG	61.7	52–61
14	F	GATCAGTTTACCCCATTTCTTCAC	58.3	52–61
	R	AGAGCAGACGCAGAAAGATGTACT	59.5	51–60
			56.6	52–64
15	F	AATGCAATTTCTGATGTGTTCAGT	59.0	54–63
	R	CAAAGCTCAAGATCCAGTCAGTAA	62.0	51–60
16	F	TTTTCAAAGCCTCTTATCAGGAC	56.2	55–64
	R	GCCTTCCATATGATCTGATAACCT	59.2	52–61
17	F	AGCTTCCAAGGACTAGGTCATTTA	60.2	53–62
	R	AATATATTCCACTGCCTCAATTCC	61.0	53–62
18	F	AACTGATGCTACTCTTCAGAGGTCTA	58.7	55–64
	R	CTCTGAAATTTCCTTCCCTTTCTC	60.5	54–63
19	F	AGTAAGTCACAGGCACCAGATACA	59.4	54–63
	R	ACCATTTTGGAATCTGCAAGTTAT	60.4	53–62
			62.8	50–59
20	F	ATGTATGTACACCCCTGCCTCT	60.3	51–60
	R	TGATACCTTCTCTAAATGCCACTG	61.3	50–59
21	F	GGTTGTGAAGAACTGGCTAAGAAT	61.0	53–62
	R	AGGCTGAAAGAAACAGTGGTAAAC	63.0	51–60

TABLE 2. PCR PRIMER SEQUENCES AND DHPLC ANALYSIS CONDITIONS (TEMPERATURE AND GRADIENT) FOR *NOTCH2* MUTATION SCREENING (CONT'D)

Exon[a]	*F/R*[b]	*Primer sequence (5'-3')*	*DHPLC temp (°C)*	*DHPLC gradient*[c] *(% B/4.5 min)*
22	F	TGGTCCAATATTTCTTGTCCTTTT	61.1	49–58
	R	AAAATCCCCTGAACACTAAGAATG		
			59.8	55–64
23	F	GGATTTTCATAATTCTGTACCTCTTC	61.2	54–63
	R	CCAATTTGTTCACTAAAACCATCC	63.2	52–61
24	F	ATTACCACAGGCCTAGAACTGAAC	57.2	55–64
	R	CAGATTGTATGGAAGAGACAATGC	62.0	50–59
			61.9	55–64
25a	F	ATATGACTGTTTTCCTACCAATGC	63.8	54–63
	R	ACAATACTGGCTCAGACAGGTG	66.5	51–60
25b	F	CTCCTTATTACTCCTGCCAGTGTG	60.5	56–65
	R	GTTAGTGACAGTCCCCTTCAGTTC	62.5	54–63
			58.8	58–67
26	F	AAATGGGTAGGAAAATCCACAGTA	59.5	57–66
	R	GGCTTCATAAAATTAGCCTTGAA	61.2	55–64
			63.0	53–62
27	F	CTGACCTGCACTCTTCTGTTTTAC	60.8	53–62
	R	GATTCATTTAGAGGGCAACTTTGA	62.5	51–60
28	F	GGGAACAATTTTCATTATGTAGCC	59.2	54–63
	R	GAGTAAATGCCCAGAGCTTAGAAT	62.0	51–60
			55.8	53–62
29	F	CCAAGACCCTGCAAAATTGTAATA	57.8	51–60
	R	CAGATAATGGCTGACAATGGTG	60.2	49–58
30	F	AGATTGATAGGGAGCATTGTTTTC	59.4	55–64
	R	ATTCATTTCCTCGAGCTGATTTAG	63.0	52–61
31	F	GGGTTAACTACCTTCTCCTTCTTG	60.1	56–65
	R	CGATAAAACATTATAGAGCCATAGGA	63.5	53–62
			64.2	52–61
			58.8	53–62
32	F	TTCATTATTTTCCTTCATCCAGGT	61.2	51–60
	R	GTAACTCTATTCCCCTCGTCAGAG	63.5	49–58
33	F	CTGGGGAGTTTAAGATTTCATTGT	60.0	49–58
	R	CAAGAGAAGCTGTAAGGAGAAACG	61.0	48–57
34a	F	GTTATTAACATGTGTTCTGTGATGG	60.3	57–66
	R	CCTTCTCACTCAGAGACTTCTTCC	61.5	56–65
34b	F	AAGAAGTCTAGACGGCCCAGT	59.8	56–65
	R	ACACAATGTGGTGGTGGGATAG	62.0	54–63
34c	F	GCCCAGCATGCACTATCTTT	61.6	57–66
	R	CATTTCTGGAATCTGGTACATGGT	62.5	56–65
			61.6	57–66
34d	F	CTGAAGGGAAGCACATAACCAC	62.6	56–65
	R	CTGACCAGTCAGAAGCAGAGTG	64.5	54–63
			61.2	54–63
34e	F	AGCACAGTTATGCTTCCTCAAAT	62.2	53–62
	R	CAGCAGCATTTACAAAAGTCAGGTT	63.5	52–61

[a]Some exons are amplified in multiple PCRs, designated a, b, etc., and some PCRs contain more than one exon.
[b]F, upstream primer; R, downstream primer.
[c]Buffer A is 0.1 *M* triethylammonium acetate; Buffer B is 0.1 *M* triethylammonium acetate containing 25% (v/v) acetonitrile. "56–65" indicates that the gradient consists of 56% B: 44% A through to 65% B: 35% A.
[d]Primers which had been used in a previously published study (McDaniell *et al.*, 2006s).

TABLE 3. PCR PRIMER SEQUENCES FOR SITE-DIRECTED MUTAGENESIS OF PREVIOUSLY DESCRIBED MUTANT ALLELES OF *NOTCH2*

Mutant alleles	*Outer forward primer*[a]	*Inner reverse primer sequence (5'-3')*[b]	*Inner forward primer sequence (5'-3')*[b]	*Outer reverse primer*[a]
1331G > A (C444Y)	exon 8 F	ACCCTTCAGATACTCACAGTGG	CCACTGTGAGTATCTGAAGGGT	exon 8 R
IVS32-1G > A	exon 33F	GAAGAGCAGATTTTCTTGCAG	CTGCAAGAAAATCTGCTCTTC	exon 33 R

[a]See Table 2 for primer sequence.
[b]Underlined nucleotide shows mismatch position.

1993; Udaka *et al.* 2005b). Briefly, two segments of a gene were independently amplified by PCR and then fused together in a subsequent reaction. Mutations were introduced into a targeted region using mutant primers containing mismatches in their central region. Because the mutant primers were complementary, the two overlapping fragments could be fused together in a subsequent extension reaction. Two PCR steps were performed to amplify two separate products using appropriate outer and inner mutated primers. PCR conditions for the primary PCR were 30 cycles of 95°C for 30 sec, 58°C for 30 sec, and 72°C for 60 sec using outer forward–inner reverse and inner forward–outer reverse primer pairs (Table 3), respectively. Then,

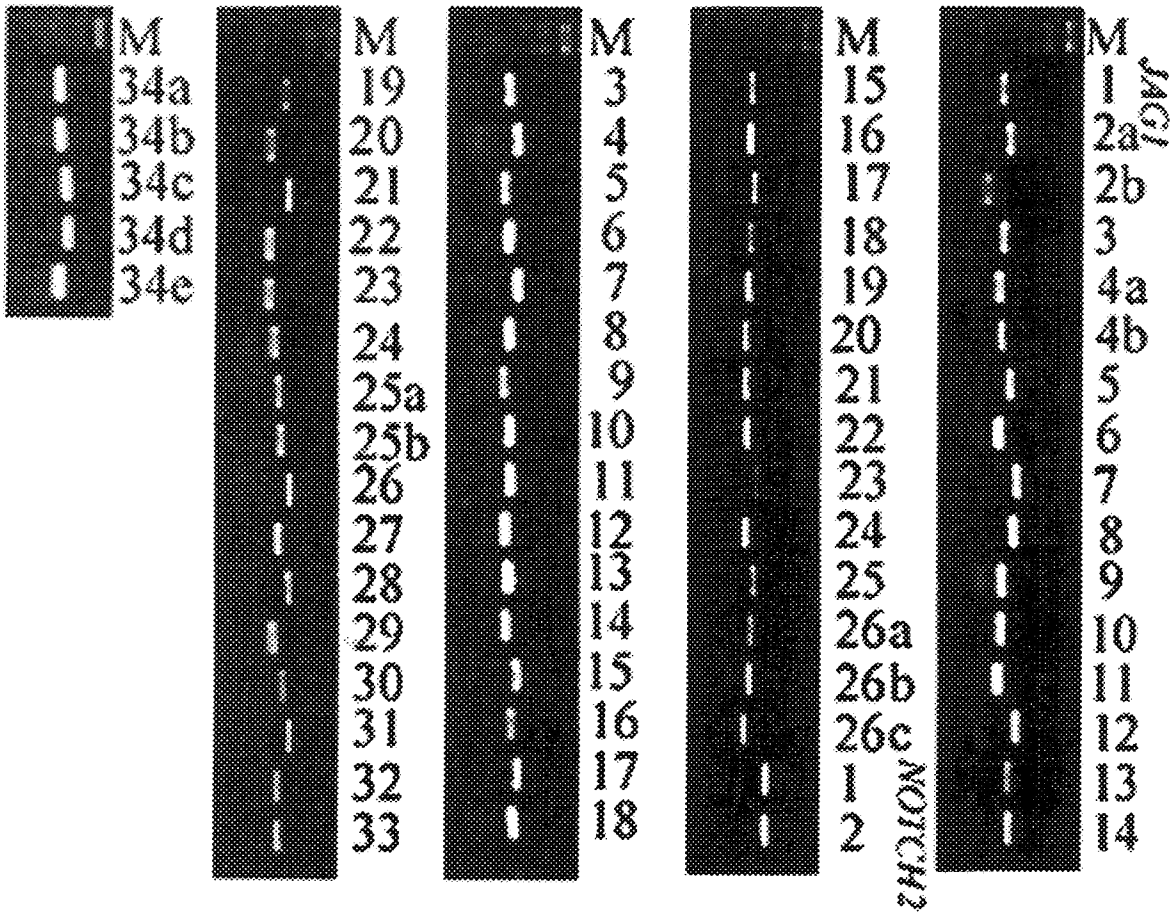

FIG. 1. PCR amplification for all coding exons of *JAG1* and *NOTCH2* using the same amplification conditions. One percent agarose gel electrophoresis of all 69 amplicons covering the entire coding regions of the two genes is shown. The leftmost lane (M) in each gel contains 1-kb ladder markers corresponding to 100-, 200-, 300-, 400-, 500-, 650-, 850-, and 1,000-bp fragments; the other lanes were loaded with 3 μL of PCR products. Please note that this figure was presented for illustrative purposes. We do not usually subject each plate to agarose gel electrophoresis prior to DHPLC analysis.

PCR products were purified by desalting column (Qiagen). Secondary PCR was performed using the outer forward and outer reverse primers and an appropriate amount of two primary PCR products as a template, using the same conditions as for the primary PCR. The PCR products were purified using a desalting column (Qiagen), sequence-verified, and used as the positive controls for the DHPLC assay.

RESULTS

Optimization of the PCR conditions

The coding regions of *JAG1* and *NOTCH2* were amplified in 30 and 39 amplicons, respectively (Tables 1 and 2). The 30 + 39 primer pairs, all with the same cycling conditions, were aliquoted on a 96-well format PCR plate. In this manner, all the exons were amplified simultaneously using a single block of a thermal cycler. The PCR plate will be referred to as the Condition-Oriented-PCR primer-Embedded-Reactor plate (COPPER plate) (Kosaki *et al.* 2005). All the exons were successfully amplified under a single condition without producing any artifacts from mispriming or primer–dimer formation (Fig. 1).

Optimization of the DHPLC conditions

The predicted optimal column temperatures and elution gradient for the DHPLC analysis of each PCR amplicon were verified by confirming that the elution profile of each of the PCR amplicons generated from wild-type genomic DNA (Kosaki *et al.* 2005; Udaka *et al.* 2005a, 2005b) had a sharp and solitary peak. The optimized column temperatures and elution gradients for the DHPLC analysis of each PCR amplicon are shown in Table 1. Figure 2 shows DHPLC profiles for the *JAG1* mutations discovered in our patient population.

Several specific factors are known to affect the sensitivity of the DHPLC assay. First, the use of impure oligonucleotide primers for PCR amplification can yield false-positive results. Second, poor quality of the DNA polymerase can also yield false-positive results (Kosaki *et al.* 2005). Third, the fragment size can affect the sensitivity of the assay; the optimal fragment size ranges from 150 bp to 700 bp (Xiao and Oefner 2001). Fourth, a high G-C content may affect the performance of the

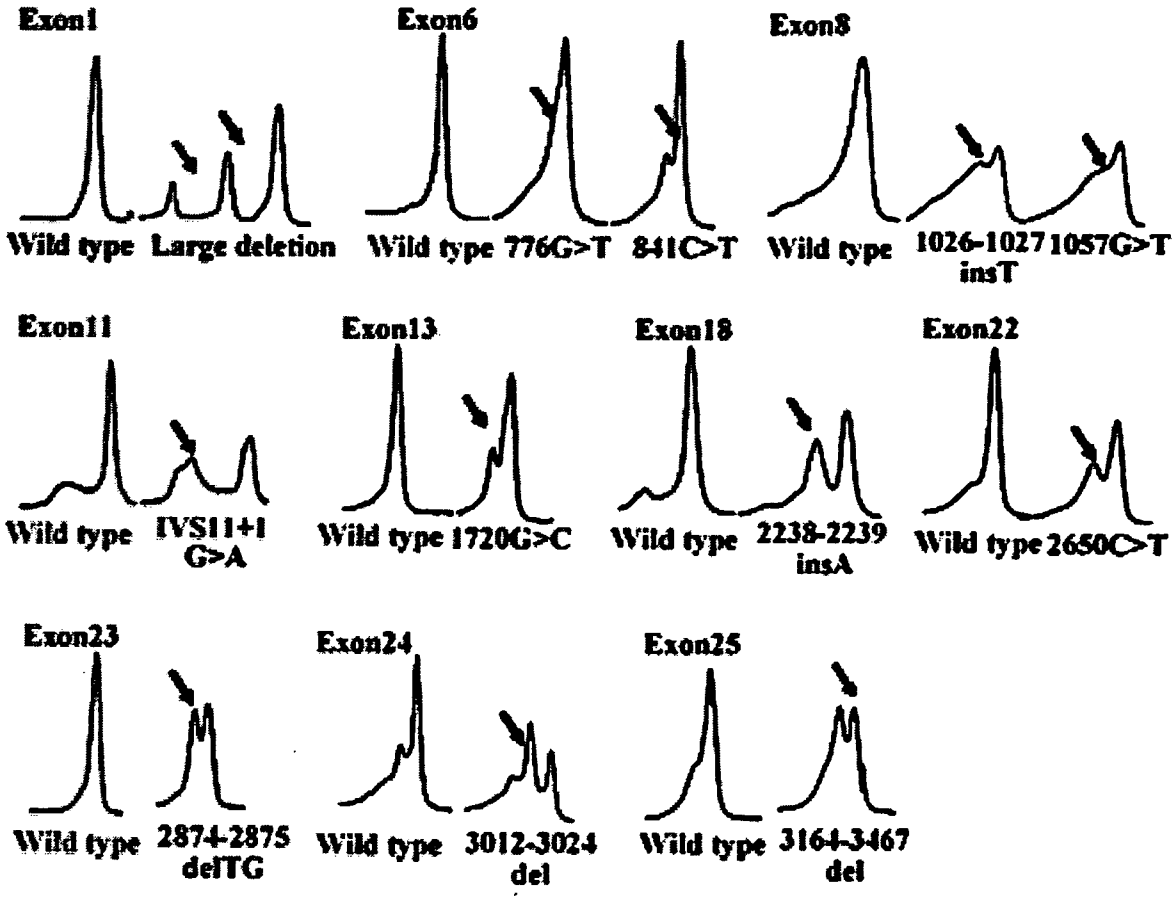

FIG. 2. DHPLC elution profiles of *JAG1* mutations detected in the present study. The column temperatures were 70.5°C, 62.7°C, 62.7°C, 53.3°C, 60.2°C, 62.8°C, 61.1°C, 61.2°C, 57.3°C, and 57.9°C for exons 1, 6, 8, 11, 13, 18, 22, 23, 24, and 25, respectively. Only the chromatogram with the best resolution of the heteroduplex peak is shown for each mutation.

TABLE 4. CLINICAL FEATURES OF THE PATIENTS WITH JAG1 MUTATION

Mutations		*Deletion including start codon*	*776G>T*	*841C>T*	*1026-10 27 insT*	*1057G>T*	*IVS11 +1G>A*	*IVS11 +1G>A*	*1720G> C*	*2238-223 9 ins A*	*2650C>T*	*2874–2875 delTG*	*3012-3024del TTCCCCTTC AGCG*	*3164–3167 delTAAG*
Location		*Exon 1*	*Exon 6*	*Exon 6*	*Exon 8*	*Exon 8*	*Intron 11*	*Intron 11*	*Exon 13*	*Exon 18*	*Exon 22*	*Exon 23*	*Exon 24*	*Exon 25*
Domain		*NAP*	*EGF1*	*EGF1*	*EGF4*	*EGF4*	*EGF10*	*EGF10*	*EGF14*	*CR*	*CR*	*C958 fs X965*	*P1004*	*V1055 fs*
Amino acid substitution		*NAP*	*G259V*	*Q281X*	*D343X*	*E353X*	*NA*	*N.A.*	*V574L*	*S747 fs*	*Q884X*		*fs1031X*	*X1061*
Sex	*Male/Female*	*F*	*M*	*M*	*F*	*F*	*M*	*F*	*F*	*755X*	*F*	*M*	*M*	*F*
age	*y m*	*Died at 12 y*	*3y 11m*	*31y*		*11y 9m*	*1y 1m*	*5y*	*0y 5 m*	*S747 fs*	*0 y 5 m*	*12y*	*8 y 5 m*	*6 y 5 m*
Craniofacial	deep set eyes	NA.V	+	−	−	+	+	+	−	+	+	+	+	−
	retrognathia /prominent chin	NAV	+	+	−	+	+	−	−	+	+	−	+	+
Ophthalmic	posterior embryotoxon	−	+	+	−	−	−	+	−	−	+	−	+	+
	iris anomaly /axenfeldt anomaly	−	−	+	−	−	−	−	−	−	−	−	+	−
	retinal degeneration	−	−	+	−	−	+	−	−	+	−	−	+	−
Cardiovascular	peripheral pulmonary stenosis	−	+	−		+	+	−	−	+	+	+	+	+
	other congenital heart defects	ASD	TOF	−	−	−	−	ASD, PS	PS	−	−	−	TOF	PDA
Hepacic	chronic cholestasis	+	+	+	+	−	+	−	+	+	+	+	−	+
	liver dysfunction	+	+	+	+	+	+	+	+	+	+	+	−	+
	GOT/GPT/TB	262/134/18.4	102/126/1.2	NAV	207/291/12	90/104/0.8	414/274/17.1	202/281/0.7	85/92/2.1	81/84/0.6	96/107/10.3	321/298/2.5	38/21/0.77	Post-trasplan-tation
	paucity of intrahepatic interlobular bile ducts	+	N.D	−	N.D	+ bilateral hypoplasia	N.D	−	+	N.D	−	+	N.D	
Renal	structural defects	−	−	−	−	−	−	−	−	−		−		
	renal failure	+	−	+	−	+	−	−	−	−	−	−	−	−
Family history		+	−	+	−	−	−	−	−	−	−	−	−	−

+: Present, −: Absent; NAP, Not applicabale; NA, not available; ND, biopsy not performed.
ASD, atrial septal defect; TOF, tetralogy of Fallot; PS, pulmonary stenosis; PD, patient ductus arteriosus.

DHPLC (Escary *et al.* 2000). We have taken all of these factors into account in the design of the assay.

The DHPLC analysis system used in the present study (Transgenomic) allowed us to write a computer script to analyze all the PCR amplicons generated from various portions of the *JAG1* gene in a serial manner at optimized conditions determined individually for each amplicon. This script enabled us to analyze the entire gene overnight in an automated manner. The complete script is available on our Website at http://www.dhplc.jp, both in text and binary format. The binary format script can be directly loaded onto the controlling units of Transgenomic DHPLC systems.

Mutation analysis of patients with Alagille syndrome

The mutations identified in the present study and the associated clinical features are summarized in Table 4. We identified heterozygous *JAG1* mutations in 13 (72%) of the 18 probands enrolled in the study, including five frameshift mutations, three nonsense mutations, two splice-site mutations, and two missense mutations, and one deletion of the 5′ end of the 5′ UTR and the coding region including the start codon. An IVS11+1G>A splicing mutation was detected in two unrelated patients. Eight of the mutations, deletion including start codon, 776G>T, 1026–1027 ins T, IVS11+1G>A, 1720G>C, 2238–2239 ins A, 2650C > T, and 3012–3024 del TTCCCCTTCAGCG have not been previously described. Known SNPs in the *JAG1* gene that are published in the dbSNP database (www.ncbi.nlm.nih.gov/projects/SNP/) were detected, including rs1051415, rs1801138, rs3178014, and rs1051419. No apparent correlation between genotype and phenotype was observed.

Nonsense mutations, as well as deletions and insertions leading to frameshifts, can unambiguously be identified as disease-causing mutations in *JAG1*. The G to A mutation that occurred at the invariant G base of the splice-donor sites flanking exons 11 is most likely pathogenic. This intronic sequence variant was not found in 100 ethnically matched controls. We further attempted to quantify the pathogenicity of these sequence variants by using the NNSplice program (http://www.fruitfly.org/seq_tools/splice.html) (Reese et al. 1997). The NNSplice program calculates the probability of splicing at a specific splicing site. The IVS11+1G>A mutation reduces the probability score from 0.98 to null. These data support the notion that the IVS11+1G>A mutation may affect normal splicing. AU2

Two heterozygous missense substitutions, G259V and V574L, were identified in exon 6 and exon 13, respectively. These missense substitutions are likely to be pathogenic because G259V and V574L residues were conserved in *Macaca mulatta*, *Mus musculus*, *Rattus norvegicus*, and *Danio rerio*, and were not found in 100 ethnically matched controls. We clinically evaluated the parents of the patient with the V574L substitution and confirmed that they showed no signs of Alagille syndrome and the parents were tested for the V574L substitution and found not to have the substitution. Hence, the V574L substitution is likely to have occurred *de novo*. A complete study to support the pathogenicity of the substitution should include a molecular genetic evaluation of the parents to confirm parentage, but the parents declined paternity testing. Because the base substitution 1720G>C leading to V574L occurred at the 3′ end of exon 13, the base substitution might have affected the splicing of intron 13. We attempted to quantify the pathogenicity of the sequence variant using the NNSplice program. The V574L mutation reduced the probability score from 0.94 to 0.5. We could not determine whether *G259V* occurred *de novo*.

In the remaining five patients, all the coding exons of *JAG1* were amplified by PCR and then sequenced in parallel, but no pathogenic mutations were identified. The possibility that the entire *JAG1* gene had been deleted was excluded in four of the five patients because each of the four patients was heterozygous for at least one SNP in the *JAG1* gene. We further screened these five patients without *JAG1* mutations for *NOTCH2* mutations using DHPLC, but no mutations were identified. In these five patients, all the coding exons of *NOTCH2* were amplified using PCR and then sequenced, but no pathogenic mutations were identified.

Known SNPs in the *NOTCH2* gene that are published in the dbSNP database (www.ncbi.nlm.nih.gov/projects/SNP/) were detected, including rs6685892, rs2604045, rs1616532, and

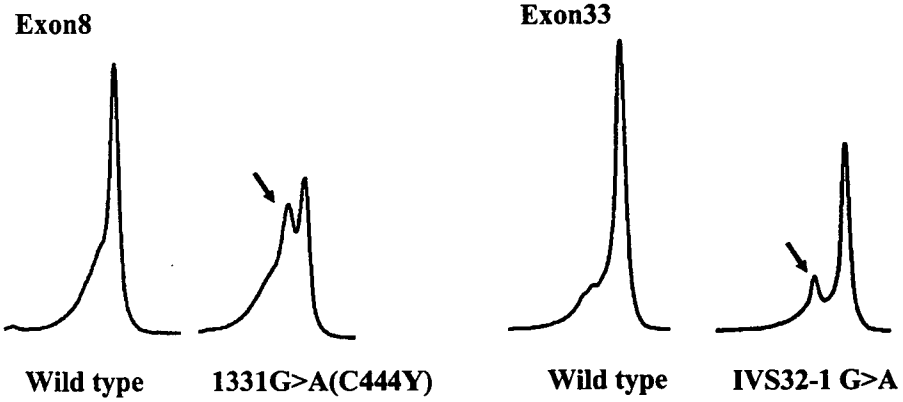

FIG. 3. DHPLC elution profiles of *NOTCH2* mutations previously described (McDaniell *et al.*, 2006). The column temperatures were 61.0°C and 60.0°C for exons 8 and 33, respectively. Only the chromatogram with the best resolution of the heteroduplex peak is shown for each mutation.